SNS LINAC HALO MITIGATION*

Dong-o Jeon[†], A. Aleksandrov, J. Wei, ORNL, Oak Ridge, TN37830, USA
J. Stovall, L. Young, H. Takeda, S. Nath, LANL, Los Alamos, NM87545, USA
R. Keller, J. Staples, LBNL, Berkeley, CA94720, USA

Abstract

The beam distribution, based on the Front End (FE) emittance measurements and multiparticle simulation studies, develops halo that leads to beam loss and radio activation of the Spallation Neutron Source Linac. A few schemes of mitigating halo were studied. Modifying the Medium-Energy Beam Transport optics and introducing adjustable collimators in the MEBT significantly reduced beam losses in the CCL, which is a preferred scheme for mitigating halo. It turns out that the DTL collimation does not effectively remove halo and presents a risk of overheating drift tubes. More thorough discussions of this matter are in press [1].

1 INTRODUCTION

The SNS Linac is designed to accelerate intense H$^-$ beams to energy of 1-GeV, delivering more than 1.4 MW (upgradeable to 2 MW) of beam power to the neutron production target [2]. Emittance measurements are made at the end of the LEBT (Low Energy Beam Transport) and the beam distribution is constructed based on the measurements. This beam is tracked though the RFQ and results in the beam shown in Fig. 1, which has a similar amount of halo as the beam originating from an initial water-bag distribution. Note that all the scattered particles are low energy ones and got lost immediately.

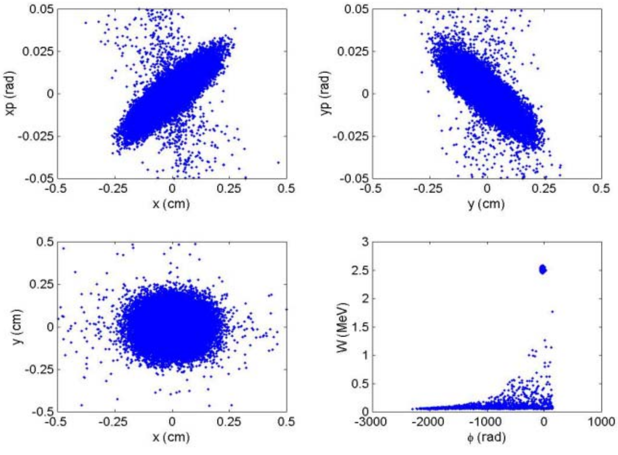

Figure 1: Projections of beam distribution at MEBT entrance. 1.4% are the low energy particles below 2MeV (scattered particles in x-px and y-py plane).

However, Fig. 2 shows the well-developed horizontal halo in transverse phase-space projections of the beam at the end of the MEBT (before the DTL), which is largely a result of the MEBT optics. The beam is tightly focused in the MEBT to facilitate beam-gap chopping. This generates large beam eccentricity and the space-charge force results in a significant beam halo [1]. In the DTL, the energy associated with the horizontal tails quickly gets redistributed, resulting in a halo in both horizontal and vertical emittance projections. We are concerned with any increase in the real-spatial size of the beam, which increases the risk of interception with the linac bore.

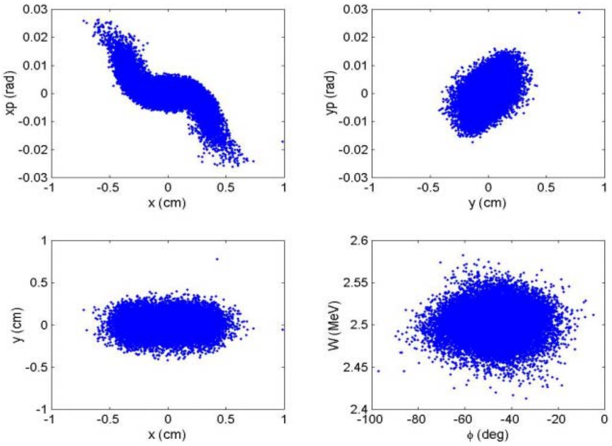

Figure 2: Projections at the end of MEBT.

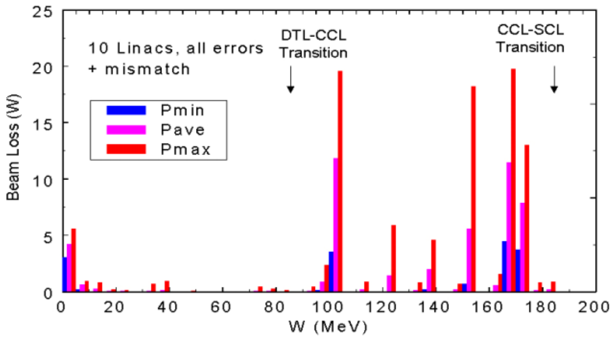

Figure 3: Beam loss plots with machine imperfections and mismatch for the original MEBT. Most beam loss takes place in the CCL and at transitions between structures.

Throughout the CCL the focusing strength of the transverse lattice gradually weakens to smoothly match the focusing strength in the Superconducting linac (SCL). As a result, the beam size is largest near the end of the CCL, so that most of the beam loss occurs at energies near 171 MeV. By including expected machine imperfections in the simulations we readily see the locations of "hot spots" caused by beam loss, as shown in Fig. 3. Ten Linac runs are made with machine imperfections. The maximum,

---

*Work supported by the DOE, under contract No. DE-AC05-00OR22725 with UT-Battelle, LLC for ORNL

[†] jeond@ornl.gov

minimum, and average beam loss are plotted as a function of energy. Most hot spots are in the CCL and there is a minor hot spot at the MEBT-DTL interface.

In order to mitigate the beam loss due to halo, we studied a few collimation schemes for MEBT and DTL structures.

2 PROPOSED SCHEMES

2.1 MEBT Scraping

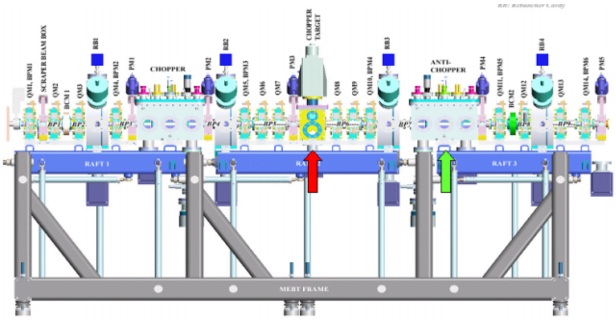

Figure 4: Schematic layout of the MEBT indicating the location of adjustable horizontal collimators at the chopper target (red arrow). A second 4-jaw adjustable collimator could replace the anti-chopper as a backup (green arrow).

There are only a few places where collimators will fit in the MEBT. One convenient place is at the chopper target. Figure 4 shows the layout of the MEBT with the chopper target and anti-chopper box indicated by arrows. The chopper target itself is located above the mid-plane to intercept beam that is deflected upward. Collimators mounted on horizontal actuators will not interfere with the function of the target. This collimator implementation has the advantage that it is readily adjustable to accommodate the actual beam conditions, which are expected to vary with different operating conditions such as beam current, ion-source performance, LEBT, RFQ, and MEBT tuning. The other advantage is that the proposed collimators can be cooled easily. The adjustable collimators are designed to scrape up to about 20% of beam power when they are made of Carbon/Carbon composite.

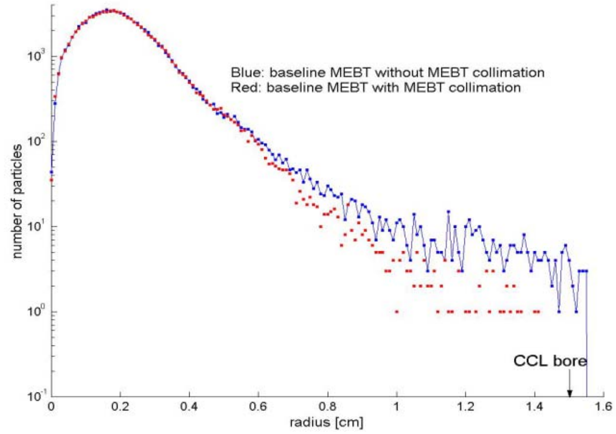

Figure 5: Beam profile at 171MeV for the baseline MEBT optics without (blue) and with (red) MEBT collimation.

We fixed the horizontal MEBT collimator aperture at ±8 mm, scraping off 2% of beam. Now there is no beam loss in an imperfection-free DTL/CCL. Figure 5 shows that, without machine imperfections, the 84% of the beam tail with r > 9 mm is removed. This result suggests that MEBT collimation at the proposed location is effective.

2.2 Alternative MEBT Optics

In an alternative design, we preserve the 90-degree phase advance from the chopper to the target, but we relax it to 63 degree downstream of the target. The resulting beam cross section is more circular as shown in Fig. 6. Now, the anti-chopper no longer restores a partially chopped portion of the beam to its original (on-axis) position in phase space, if indeed that were desirable. Also, the beam now has a larger vertical extent and, by design, approaches the anti-chopper plates more closely. Alternative modes of anti-chopper operation are under study.

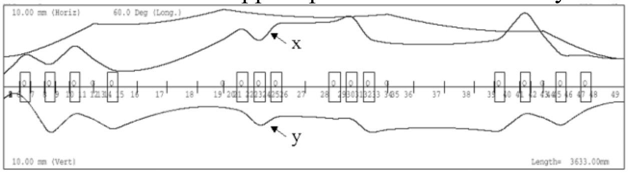

Figure 6: Trace3D beam envelope profiles of the modified MEBT optics yielding a more circular cross section in the anti-chopper.

This simple modification to the optics alone reduces the formation of transverse tails substantially and improves the beam quality in the downstream linac as is shown in Fig. 7. A simulation shows that 87% of the beam tails with r > 9 mm at 171MeV is removed. The halo reduction is comparable to the effect of MEBT collimation with the baseline MEBT optics.

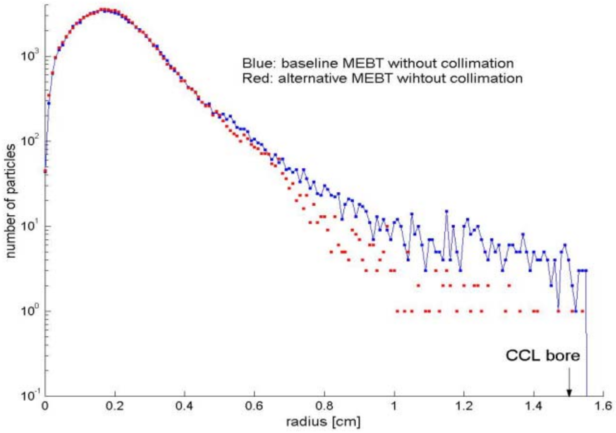

Figure 7: Beam profile at 171MeV for the baseline MEBT optics without collimation (blue) and for the alternative MEBT optics without collimation (red).

2.3 Hybrid Halo Reduction Solution

We also investigated the effectiveness of adding MEBT collimation in combination with the alternative optics design. In this scenario, we added MEBT collimation at the two locations indicated by arrows in Fig. 4. Figure 8 shows the radial beam distribution at 171 MeV resulting from this hybrid solution. 97% of the halo with r > 9 mm is removed compared with the baseline case. We also studied the effectiveness of the proposed scheme for the increased peak current of 54mA rather than 38mA. There is also enough safety margin even for this case.

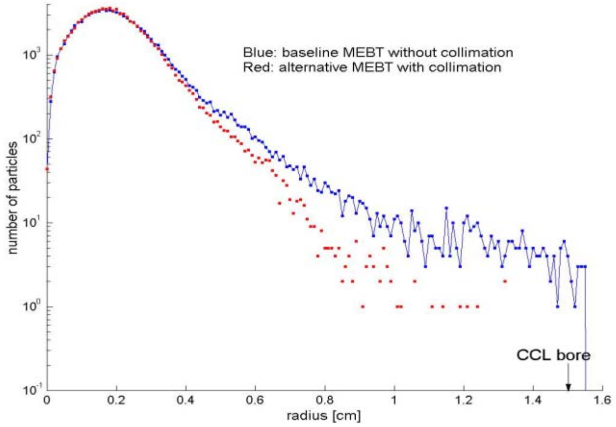

Figure 8: Beam profile at 171MeV for the baseline MEBT optics without collimation (blue) and for the alternative MEBT optics with MEBT collimation (red).

3 DTL COLLIMATION

We also explored the possibility of DTL collimation of the SNS linac. The original MEBT is used without optics modification in the tracking studies, in order to assess the effectiveness of the beam collimation in the DTL. The focusing lattice in the DTL is FFODDO, where O means empty drift tubes. We considered inserting circular collimators in the first 11 empty drift tubes. The bore radius of drift tubes is 12.5 mm. By using only empty drift tubes (white rectangles indicated by red arrows Fig. 9), we avoid the possibility of overheating and possibly approaching the Curie point of the permanent-magnet quadrupole lenses (PMQs). In addition, the beam is nearly round in the empty drift tubes making collimation by circular collimators more effective.

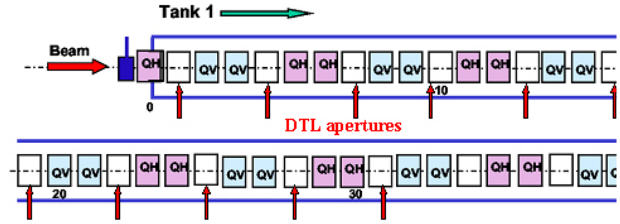

Figure 9: Schematic diagram of DTL tank 1 showing the location of proposed collimators.

We first considered 8-mm-radius circular collimator and transported the beam without including machine imperfections such as misaligned drift tubes. The collimators reduce the bore cross section by 36%, but trim just 0.22% from the beam. The left-hand plot of Fig. 10 is the expected power deposited in the collimating drift tubes. The maximum power of ~5 W deposited in drift tube 10 adds 10% to the rf heat load. The right-hand plot summarizes the simulated particle dynamics in 100 linacs that included random alignment errors. The plot shows the maximum and minimum power lost at each circular collimator. The maximum power, again at drift tube 10, was 31W, adding 65% to rf heating. However, halo collimation is poor.

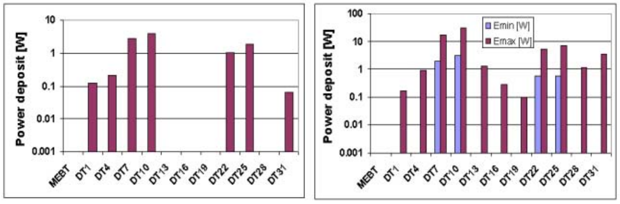

Figure 10: Power dissipation in drift tubes for 8mm-aperture DTL collimators.

6-mm apertures are used leading to reasonable halo collimation. The left-hand plot of Fig. 11 shows that, excluding machine imperfections, the beam power deposited in drift tube 10 would double the design thermal load. Including machine imperfections (right-hand plot), the maximum expected power deposited in drift tube 22 is 444 W, which is ~6 times the design cooling capacity of this drift tube.

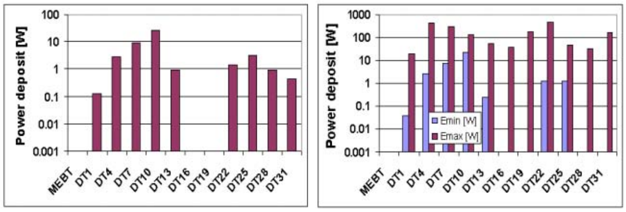

Figure 11: Power dissipation in drift tubes for 6mm-aperture DTL collimators.

4 CONCLUSIONS

After investigating the potential for mitigating halo by introducing apertures in the DTL, we conclude that this scheme is not effectively removing halo. Too small an aperture is required to reduce halo significantly, and results in severe thermal loading of the drift tubes. Fixed apertures would limit our ability to accommodate any variety of beam conditions.

Modifying the MEBT optics and introducing adjustable scrapers as needed is a preferred alternative for mitigating halo by pre-empting its formation. The hybrid solution does not involve any redesign that would impact the construction schedule. Because the lenses and scrapers are all adjustable, this scheme is adaptable to any operational scenario.

5 REFERENCES

[1] Dong-o Jeon et al, “Formation and Mitigation of Halo Particles in the Spallation Neutron Source Linac”, in press.

[2] Norbert Holtkamp, “The SNS Linac and Storage Rings: Challenges and Progresses Towards Meeting Them”, Proceedings of EPAC 2002, June 2002.